

Domain formation in the structural phase transition of the organic superconductor κ_L -(DMEDO-TSeF)₂[Au(CN)₄](THF)

Tadashi Kawamoto*

Department of Organic and Polymeric Materials, Graduate School of Science and Engineering, Tokyo Institute of Technology, O-okayama, Meguro-ku, Tokyo 152-8552, Japan

Takehiko Mori

Department of Chemistry and Materials Science, Graduate School of Science and Engineering, Tokyo Institute of Technology, O-okayama, Meguro-ku, Tokyo 152-8552, Japan

Toru Kakiuchi

Department of Materials Structure Science, The Graduate University for Advanced Studies, Ibaraki 305-0801, Japan

Hiroshi Sawa

Department of Materials Structure Science, The Graduate University for Advanced Studies, Ibaraki 305-0801, Japan and Institute of Materials Structure Science, High Energy Accelerator Research Organization, Ibaraki 305-0801, Japan

Takashi Shirahata, Megumi Kibune, Hiroko Yoshino, and Tatsuro Imakubo
Imakubo Initiative Research Unit, RIKEN, Hirosawa, Wako, Saitama 351-0198, Japan

(Received 19 June 2007; published 31 October 2007)

Structural properties of the layered organic superconductor κ_L -(DMEDO-TSeF)₂[Au(CN)₄](THF) have been investigated, where DMEDO-TSeF is dimethyl(ethylenedithio)tetraselenafulvalene. We have found that a structural phase transition occurs at $T_d=209$ K, and that only the (0 0 *l*) Bragg reflections split into two along the b^* direction below T_d . The low-temperature structure is composed of two monoclinic domains with the space group $P2_1/n11$. The low-temperature monoclinic phase has two crystallographically independent dimers in a conducting layer, suggesting that the present compound potentially borders on the checkerboard-type charge ordered state, and has possibly different symmetry of superconductivity from the ordinary κ -type superconductors.

DOI: [10.1103/PhysRevB.76.134517](https://doi.org/10.1103/PhysRevB.76.134517)

PACS number(s): 74.70.Kn, 61.50.Ks

I. INTRODUCTION

Most organic superconductors have been obtained as clean single crystals; the donor molecules and anions are in ordered states.¹ Recently, two organic superconductors with the same composition, κ_L - and κ_H -(DMEDO-TSeF)₂[Au(CN)₄](THF) as shown in Fig. 1, have been developed.² The space group of the high- T_c phase (H phase: onset $T_c=4.8$ K) is $P2_1/c$ and that of the low- T_c phase (L phase: onset $T_c=3.0$ K) is $Pnma$. The donor arrangement of these materials, however, is basically the same κ -type structure. In the κ -type donor arrangement, the donor molecules form face-to-face and head-to-tail orthogonal dimers; that is, they are rotated by approximately 90° with respect to each other [Fig. 1(b)]. The conducting layer of the L phase is on the crystallographic ac plane, and that of the H phase is on the bc plane. For both compounds, the unit cell contains two conducting sheets. The L phase has one crystallographically independent conducting layer, but the H phase has two independent layers. Although the solvent molecule tetrahydrofuran (THF) of the H phase is ordered even at room temperature, THF of the L phase is disordered by the mirror symmetry as shown in Figs. 1(c) and 1(d). In the transport properties, the H phase shows simple metallic behavior below room temperature. The electrical resistance of the L phase increases with decreasing temperature below

room temperature, and decreases below about 110 K.

Among organic superconductors, the κ -type materials have a strongly correlated electronic state. In this type, the antiferromagnetic Mott insulating state changes to a superconducting phase by applying pressure. This phase diagram, called Kanoda's diagram, is well explained by the strength of the electronic correlation,³ and the higher T_c materials show the larger ratios of the observed to the bare cyclotron masses.⁴ In the usual κ type, all dimers are equivalent, and all conducting layers are equivalent.

There are several organic superconductors including organic solvent molecules. κ_L -(BEDT-TTF)₂ M (CF₃)₄TCE [BEDT-TTF: bis(ethylenedithio)tetrathiafulvalene, $M=Cu$, Ag, and Au, TCE: 1,1,2-trichloroethane] is in this category.⁵ Although there are two phases (the H and L phases), the crystal structure has been solved only for the L phase.^{6,7} Therefore, the relation between the structure and superconductivity has not been studied. On the other hand, the DMEDO-TSeF superconductors are good materials to investigate the relation between the superconductivity and the slightly different structures.

The present paper reports the structural phase transition of κ_L -(DMEDO-TSeF)₂[Au(CN)₄](THF); the orthorhombic system changes to two monoclinic domains below 209 K. The low-temperature monoclinic phase, which has the same symmetry as that of the checkerboard-type charge order, is

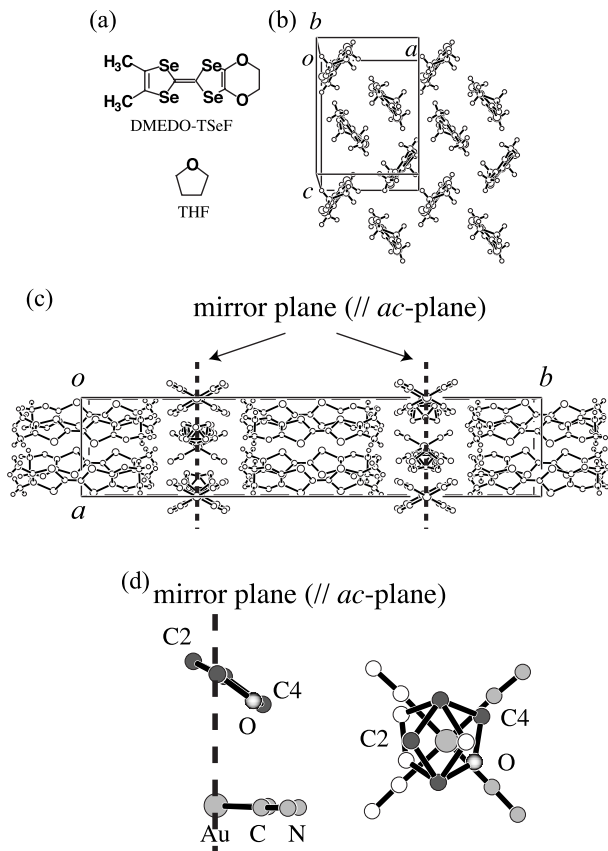


FIG. 1. (a) DMEDO-TSeF and THF molecules. (b) Crystal structure of the L phase projected along the molecular long axis. (c) Projection onto the ab plane. (d) The anion and solvent molecules. The left side shows crystallographically independent parts. The right side shows the solvent disordered by the mirror plane.

the first superconductor of this type of the κ structure.

II. EXPERIMENT

High quality single crystals were prepared by electrocrystallization in RIKEN.² The x-ray oscillation photographs were taken by an imaging plate with Si monochromated synchrotron radiation ($\lambda=1.1271 \text{ \AA}$) at BL-1B of the Photon Factory, KEK, Tsukuba. The x-ray diffraction measurements were made on a Rigaku AFC7R four-circle diffractometer with graphite monochromated Mo $K\alpha$ radiation and a rotating anode generator ($\lambda=0.71069 \text{ \AA}$). For the low-temperature x-ray measurements, the sample was cooled down to 110 K by a nitrogen gas-stream cooling method. A sample was mounted on a glass capillary using a small amount of an Apiezon grease H mixed with an Apiezon grease N.

III. RESULTS

Figure 2 shows synchrotron radiation x-ray oscillation photographs. The photograph at 200 K clearly displays a Bragg spot splitting into two spots along the b^* direction of the prototype lattice. This split recovers to normal Bragg spots at 220 K. Therefore, the splitting of the Bragg spots

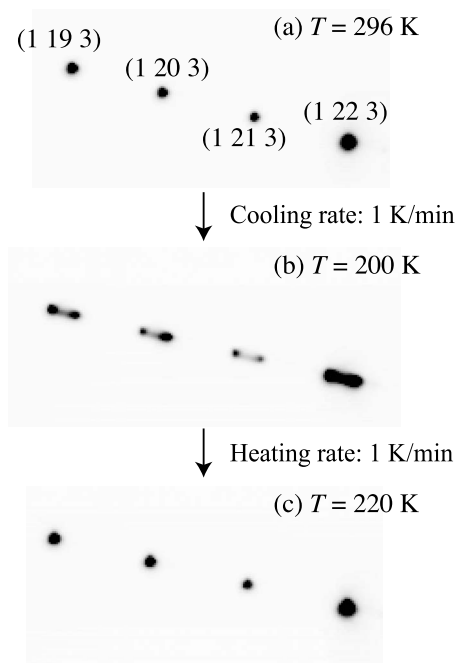


FIG. 2. Synchrotron radiation x-ray oscillation photographs at (a) 296, (b) 200, and (c) 220 K.

indicates the existence of a reversible structural phase transition in the temperature region $200 < T < 220 \text{ K}$.

In order to determine the lattice system and the phase transition temperature, x-ray diffraction measurements were carried out using a four-circle diffractometer. Figure 3 shows several peak profiles at high and low temperatures and the relation between the scan directions and the reciprocal lattice. A clear peak splitting is observed in the $(0\ 0\ 2)$ reflection only along the b^* axis of the prototype lattice. The splitting does not occur in either the $(0\ k\ 0)$ or $(h\ 0\ 0)$ reflections along either of the two vertical axes. For example, $(0\ 10\ 0)$ and $(-4\ 0\ 0)$ reflections are shown in Fig. 3. These observations show that only the interaxial angle α deviates from 90° , and the low-temperature structure is composed of two monoclinic domains; the c^* axis tilts in the b^*c^* plane of the prototype reciprocal lattice as shown in Fig. 3(d). In the real space, the present phase transition is interpreted by the tilt of the b axis in the $\{1\ 0\ 0\}$ plane, i.e., in the bc plane of the prototype lattice.

The distortion angle δ defined as $\delta = |\alpha - 90^\circ|$ is estimated as $\delta = 1.21(2)^\circ$ at 110 K from the splitting of the peak profile of the $(0\ 0\ 2)$ reflection [Fig. 3(a)]. The integrated intensity ratio of domain 1 to domain 2 directly gives a volume ratio of the two domains as approximately 52:48, almost 1:1, in the present experiment. The linewidths of the peak profiles defined as full width at half maximum give us the correlation lengths. The correlation length along the b^* direction of the prototype phase of the domain 1 is $\lambda_{k1} = 515 \text{ \AA}$ and that of the domain 2 is $\lambda_{k2} = 538 \text{ \AA}$ at 110 K. On the other hand, the correlation lengths estimated from the $(0\ 10\ 0)$ reflection are $\lambda_h = 418 \text{ \AA}$ and $\lambda_l = 156 \text{ \AA}$, respectively.

The high-temperature orthorhombic component, that is the central component in the $(0\ 0\ 2)$ peak profile, disappears at 110 K as shown in Fig. 3(a). The 110 K peak profile,

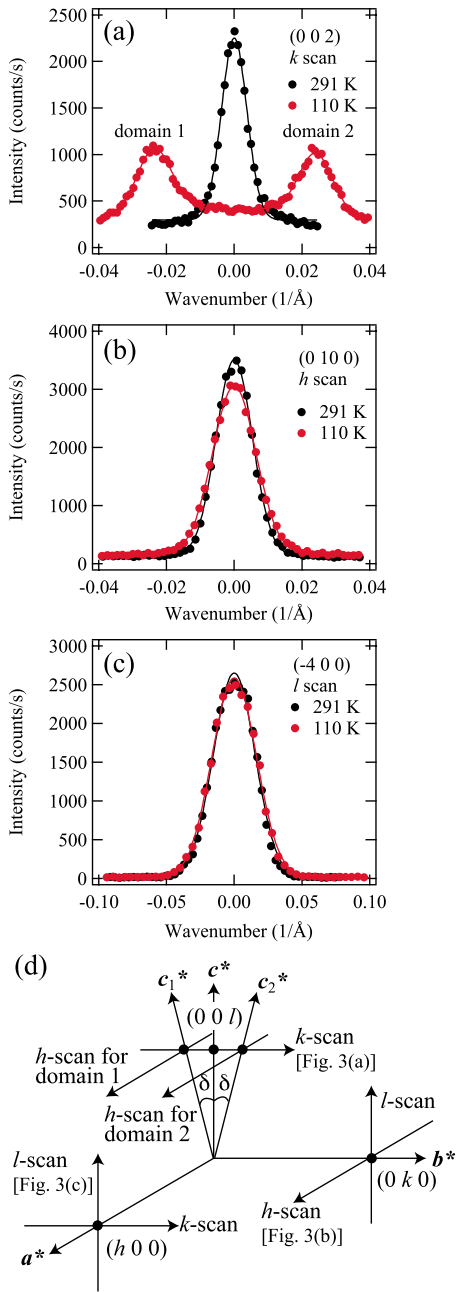


FIG. 3. (Color online) High- and low-temperature peak profiles obtained by different scan directions along the h , k , and l axes. The sample is different from that in Fig. 2. (a) (0 0 2) reflection along the b^* axis, (b) (0 10 0) reflection along the a^* axis, and (c) (-4 0 0) reflection along the c^* axis. (d) Schematic representation of the relation between the hkl scan and the reciprocal lattice.

however, shows sample dependence as shown in Fig. 4. There are clearly three components at 110 K; both the high-temperature orthorhombic and the low-temperature monoclinic phases coexist. The sample dependence of the peak profiles of the (0 0 2) reflection at 110 K means that the phase transition is very sensitive to the sample mounting, i.e., physical stress or pressure. The temperature dependence of the peak profiles of the (0 0 2) reflection shows that the splitting width decreases with increasing temperature.

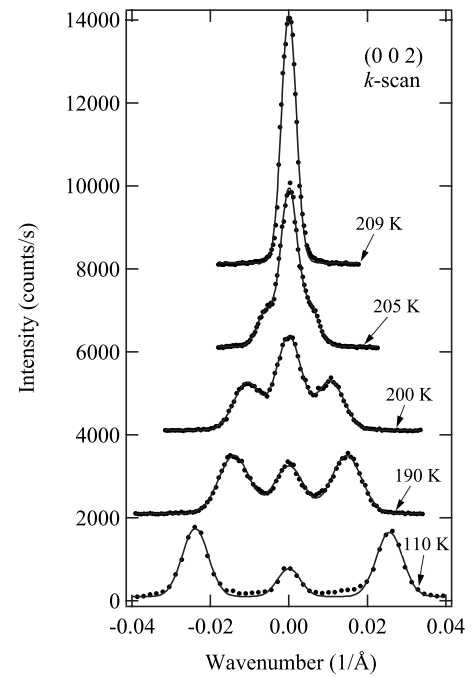


FIG. 4. Temperature dependence of the peak profiles of the (0 0 2) reflection obtained by the k scan in the heating process. The sample differs from that in Fig. 3. The top data set is fitted with a single Gaussian line shape. The other data sets are fitted assuming three components.

The distortion angle δ depends on the temperature as shown in Fig. 5(a), and δ is zero at the orthorhombic-monoclinic distortion temperature, $T_d=209$ K. The behavior of δ near T_d shows $|(T-T_d)/T_d|^{1/2}$ dependence. The temperature dependence of the integrated intensity ratio between the monoclinic domains and all components, $S_{\text{monoclinic}}/S_{\text{total}}$, gives the volume ratio as shown in Fig. 5(b). This quantity rapidly decreases near T_d with increasing temperature.

IV. DISCUSSION

The low-temperature x-ray oscillation photographs do not show any superlattice structure. Among the six kinds of peak profiles, the h and k scans of (0 0 l), the k and l scans of (h 0 0), and the l and h scans of (0 k 0), only the k scan of (0 0 l) gives a split peak profile. This indicates that the b_0 axis tilts in the b_0c_0 plane in the real space as shown in Fig. 6, where we express the prototype axes as a_0 , b_0 , and c_0 . As a result, the symmetry elements related to the b_0 and c_0 axes in the space group $Pnma$, those are the mirror plane, the a -glide plane, and two 2_1 screw axes, disappear. Therefore, the possible highest symmetrical space group of the low-temperature phase is $P2_1/n11$. The domain wall orientations are estimated by Sapriel's theory.⁸ The possible domain walls are only two, a_0c_0 and a_0b_0 planes. The peak profiles at 110 K indicate that the only one domain wall, which is parallel to the a_0c_0 plane, exists as shown in Fig. 6.

Group theory gives us a correct space group at low temperature from the experimental results.^{9,10} The point group of the disordered parent phase will be represented by G , of

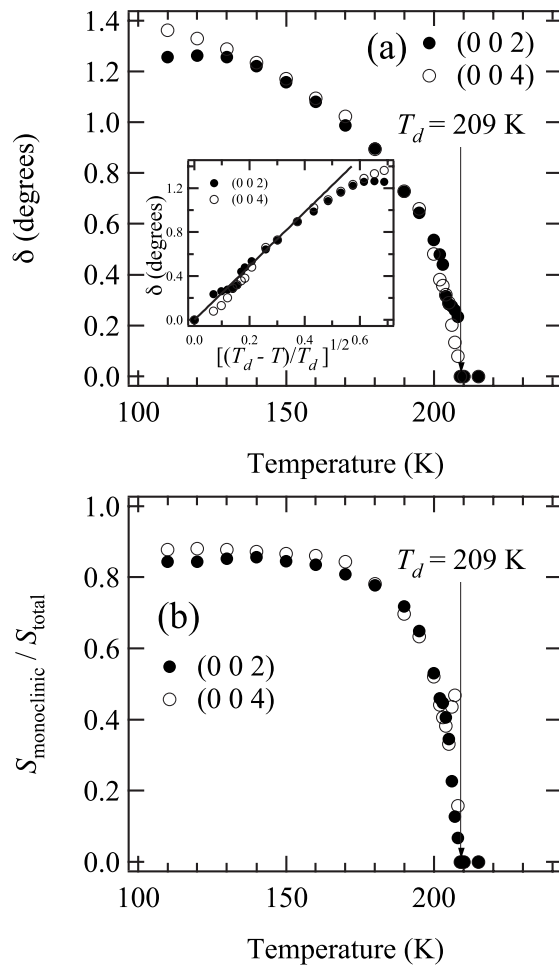


FIG. 5. (a) Temperature dependence of the distortion angle δ defined by $|\alpha - 90^\circ|$. The inset shows $\delta(\sqrt{(T_d - T)/T_d})$, and the solid line demonstrates $\delta \propto \sqrt{(T_d - T)/T_d}$ behavior. (b) The integrated intensity ratio between the monoclinic phase and all components.

order p . The ordering is usually accompanied by a decrease in symmetry in such a way that the point group of the ordered structure H of order q is a subgroup of G , i.e., $H \subset G$. Group-theoretical consideration shows that the number of variants is given by $n = p/q$. In the present compound, the high-temperature space group is $Pnma$ whose point group G is D_{2h} of order $p = 8$. The number of observed variants is $n = 2$. Therefore, the low-temperature space group is $P2_1/n11$ whose point group H is C_{2h} of order $q = 4$. We have checked the extinction rule for the n -glide symmetry by $(0 k l)$ reflections and for the twofold screw symmetry by $(h 0 0)$ reflections. The symmetry along the a_0 axis, $2_1/n$, is not destroyed by the phase transition.

The structural phase transition removes the mirror symmetry; this indicates that the THF molecules are ordered. The driving force of this phase transition is the solvent molecule ordering, so-called order-disorder transition. DMEDO-TSeF molecule has an ethylene group, the right-side six-membered ring in Fig. 1(a), and the conformation of this ring is thermally disordered in the general positions at room temperature like a BEDT-TTF molecule.² This disorder is also observed in the neutral DMEDO-TSeF crystal. In the neutral

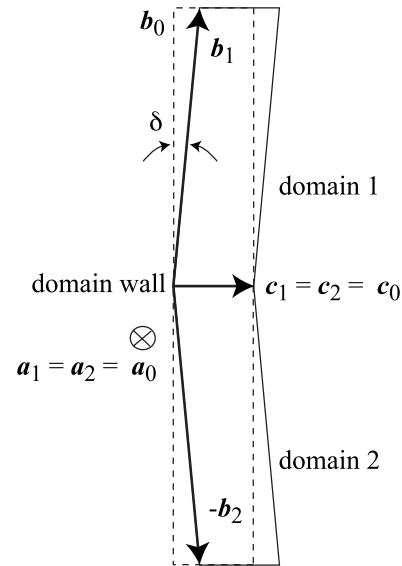


FIG. 6. Schematic representation of the twinning structure. The domain wall, that is, twin plane, is parallel to the $\{0 1 0\}$ plane, i.e., the ac plane of the prototype lattice.

crystal, the ring conformation goes to an ordered state in the temperature range $150 < T < 200$ K without any superstructure or symmetry lowering.¹¹ This indicates that the ring conformation ordering is not a phase transition but a crossover. Therefore, our detected structural phase transition is originated in the solvent molecule ordering. NaV_2O_5 also shows an orthorhombic-monoclinic distortion phase transition below $T_d = 34$ K.^{12,13} This phase transition is a charge ordering that involves a valence change of V ions, and is an insulator-insulator phase transition. The driving force of the phase transition of NaV_2O_5 is different from that of $\kappa\text{-L}(\text{DMEDO-TSeF})_2[\text{Au}(\text{CN})_4](\text{THF})$.

In the high-temperature orthorhombic phase of the L phase, there is one crystallographically independent donor molecule, the A molecule as shown in Fig. 7(a). The low-temperature phase has two crystallographically independent donor molecules, A and B in Fig. 7(b), in the same donor layer. This structure is, however, different from $\kappa\text{-(BEDT-TTF)}_2\text{Cu}(\text{NCS})_2$, which belongs to another low-symmetry space group ($P2_1$),¹⁴ and the dimer is composed of two independent molecules, A and B [Fig. 7(c)]. The conducting layer of the $\text{Cu}(\text{NCS})_2$ salt has 2_1 screw axes, but does not have any inversion center. On the contrary, the present compound has two independent dimers, the A-A and B-B pairs, in a conducting layer [Fig. 7(b)]. The present type has inversion centers but does not have 2_1 screw axes in the conducting layer. This type of κ structure has been observed in very limited materials, $\kappa\text{-(BEDT-TTF)}_4\text{PtCl}_6 \cdot \text{C}_6\text{H}_5\text{CN}$ and $\kappa\text{-(BEDT-TTF)}_4[M(\text{CN})_6][\text{N}(\text{C}_2\text{H}_5)_4] \cdot n\text{H}_2\text{O}$ ($M = \text{Co}, \text{Fe}; n = 2, 3$).¹⁵⁻¹⁷ If the A and B molecules have different charge, this type of κ arrangement potentially shows checkerboard-type charge order, and these κ -type BEDT-TTF salts actually show charge ordering.^{15,17,18} These BEDT-TTF compounds are insulators at low temperatures, but the present L phase is the first compound showing superconductivity. Although the usual κ -type superconductors in Kano-

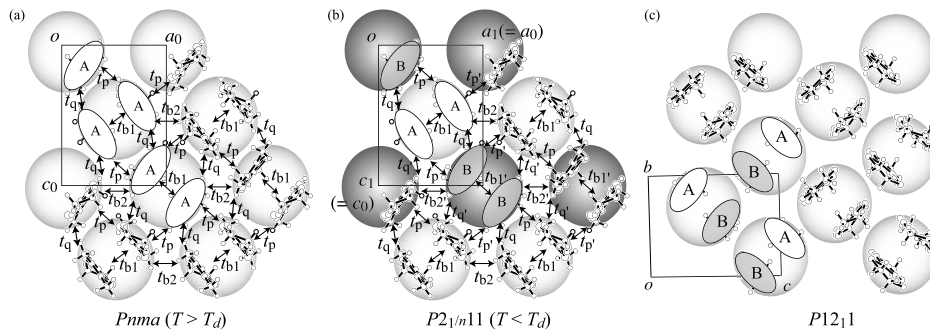


FIG. 7. Schematic drawing of the donor arrangement of κ -(DMEDO-TSeF)₂[Au(CN)₄](THF) both at (a) $T > T_d$ and at (b) $T < T_d$, and (c) that of κ -(BEDT-TTF)₂Cu(NCS)₂. A shaded circle means a dimer.

da's phase diagram border on an antiferromagnetic Mott insulating state,³ the present L-phase superconductor is potentially located next to the checkerboard-type charge ordered state. This suggests that the origin and symmetry of the superconductivity of the present compound differ from those of the usual κ -type superconductors. Interestingly, the H phase of the present compound with the same composition is possibly located in the usual Kanoda diagram. If the insulating phase bordering upon the superconducting phase is related to the symmetry of the superconductivity, there is a possibility that the superconducting symmetry of the H phase differs from that of the L phase instead of the same composition.

The Fermi surface (FS) of the κ -type organic superconductors is composed of the overlapping cylinders and there are fundamental α and β orbits as shown in Fig. 8(a). For κ -(BEDT-TTF)₂Cu(NCS)₂, the β orbit has small gaps at the zone boundary because of the crystallographic symmetry, and this orbit becomes a magnetic breakdown orbit.²² The degeneracy of the energy bands on the zone boundary occurs when the crystal has glide planes or screw axes having translation perpendicular to the boundary.²³ This is fundamentally equivalent to the extinction rule of the Bragg reflections. The energy band of the high-temperature orthorhombic phase of the L phase is degenerated on the A zone boundary [Fig. 8(a)]. Although the low-temperature monoclinic phase of the L phase has the n -glide symmetry giving the degenerated W zone boundary, this symmetry operation creates molecules in

another donor layer in the unit cell. The conducting sheet composed of two independent dimers having eight kinds of transfer integrals [Fig. 7(b)]. Therefore, the energy gap opens at the W line as shown in Fig. 8(b) for the low-temperature monoclinic phase. In contrast, the FS of the H phase is similar to that of the high-temperature L phase. However, there are two independent FS's because of two independent conducting layers. These differences will be observed in the quantum oscillation phenomena such as the de Haas-van Alphen and Shubnikov-de Haas oscillations.

We should mention the relation between the structural correlation lengths and the Ginzburg-Landau (GL) coherence lengths in the superconducting phase. The correlation length of the monodomain along the b^* axis of the prototype phase, interlayer direction, $\lambda_{\perp} \sim \sqrt{\lambda_{k_1}\lambda_{k_2}} \sim 530 \text{ \AA}$ is much longer than the GL coherence length estimated from the resistive upper critical fields, $\xi_{\perp} = 17.8 \text{ \AA}$ at 30 mK,²⁴ which is shorter than the interlayer spacing ($d \sim b/2 \sim 19.3 \text{ \AA}$ at room temperature). The short interlayer GL coherence length ($\xi_{\perp} < d$) indicates that the domain walls parallel to the $\{0\ 1\ 0\}$ plane will not affect the superconducting state. On the other hand, the intralayer correlation length, $\lambda_{\parallel} \sim \sqrt{\lambda_{\parallel}\lambda_{\parallel}} \sim 260 \text{ \AA}$, is comparable with the intralayer coherence length, $\xi_{\parallel} = 344 \text{ \AA}$.²⁴ Since there is no domain wall parallel to the $\{0\ 0\ 1\}$ plane, the domain structure of the present compound will not affect the superconducting properties. It should be mentioned that in the high- T_c superconductor La_{2-x}Ba_xCuO₄ the fraction of the low-temperature tetragonal phase correlates with T_c .²⁵ Recently, we have found that the resistive superconducting transition temperature of κ_L -(DMEDO-TSeF)₂[Au(CN)₄](THF) depends on the sample. This might be related to the sample dependence of the fraction of the monoclinic domains, $S_{\text{monoclinic}}/S_{\text{total}}$, as shown in Fig. 5(b). Although this parameter is 1.0 at 110 K for the samples in Figs. 2 and 3, that of the sample in Fig. 5 is about 0.8.

In the organic superconductor (TMTSF)₂ClO₄, where TMTSF is tetramethyltetraselenafulvalene, the Cl atoms are located on an inversion center and the oxygen atoms randomly occupy eight nearly equivalent positions at room temperature.²⁶ Although (TMTSF)₂ClO₄ shows an anion ordering phase transition, which is a kind of order-disorder transitions, at $T_{AO} = 24 \text{ K}$,²⁷ this transition does not make domain structures. Moreover, in organic superconductors with three components, donor, anion, and solvent molecules,

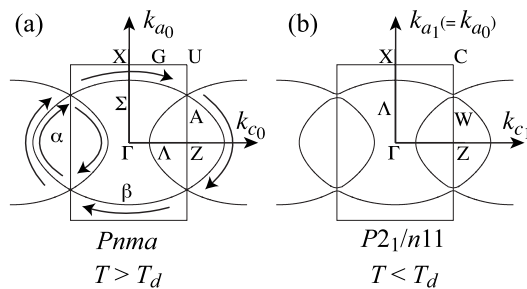


FIG. 8. Schematic drawing of the Fermi surfaces both at (a) $T > T_d$ and at (b) $T < T_d$. The FS in (a) is calculated based on the room temperature atomic coordinates (Refs. 19 and 20). The BSW symbol of the Brillouin zone changes from (a) orthorhombic system to (b) monoclinic one (Ref. 21).

κ_L -(BEDT-TTF)₂M(CF₃)₄TCE has also disordered anion and solvent molecules at room temperature. In this compound, no structural phase transition has been observed above 115 K.⁷ To the best of our knowledge, κ_L -(DMEDO-TSeF)₂[Au(CN)₄](THF) is an ambient pressure organic superconductor with domain structures.

V. CONCLUSION

κ_L -(DMEDO-TSeF)₂[Au(CN)₄](THF) shows the orthorhombic-monoclinic distortion transition below $T_d = 209$ K, and the low-temperature structure is composed of two monoclinic domains with the space group $P2_1/n11$. The low-temperature monoclinic phase has different symmetry

from the usual κ -type. The present compound is an organic superconductor with the domain structure and such a κ -type arrangement. The interlayer correlation length is longer than the interlayer GL coherence length; the domain walls will not affect the superconductivity.

ACKNOWLEDGMENTS

This work was performed under the approval of the Photon Factory Program Advisory Committee (Proposal No. 06G248), and was partially supported by a Grant-in-Aid for Young Scientists (B) (No. 19740202) and a Grant-in-Aid for Scientific Research on Priority Areas of Molecular Conductors (No. 15073211) from MEXT.

*kawamoto@o.cc.titech.ac.jp

- ¹For a review, see T. Ishiguro, K. Yamaji, and G. Saito, *Organic Superconductors*, 2nd ed. (Springer, Berlin, 1998).
- ²T. Shirahata, M. Kibune, and T. Imakubo, Chem. Commun. (Cambridge) **2006**, 1592.
- ³K. Kanoda, Hyperfine Interact. **104**, 235 (1997); J. Phys. Soc. Jpn. **75**, 051007 (2006).
- ⁴T. Kawamoto and T. Mori, Phys. Rev. B **74**, 212502 (2006).
- ⁵For a review, see J. A. Schlueter, U. Geiser, A. M. Kini, H. H. Wang, J. M. Williams, D. Naumann, T. Roy, B. Hoge, and R. Eujen, Coord. Chem. Rev. **190-192**, 781 (1999).
- ⁶J. A. Schlueter, J. M. Williams, U. Geiser, J. D. Dudek, M. E. Kelly, S. A. Sirchio, K. D. Carlson, D. Naumann, T. Roy, and C. F. Campana, Adv. Mater. (Weinheim, Ger.) **7**, 634 (1995).
- ⁷U. Geiser, J. A. Schlueter, J. M. Williams, D. Naumann, and T. Roy, Acta Crystallogr., Sect. B: Struct. Sci. **51**, 789 (1995).
- ⁸J. Sapriel, Phys. Rev. B **12**, 5128 (1975).
- ⁹G. Van Tendeloo and S. Amelinckx, Acta Crystallogr., Sect. A: Cryst. Phys., Diffr., Theor. Gen. Crystallogr. **30**, 431 (1974).
- ¹⁰V. Janovec, V. Dvorak, and J. Petzelt, Czech. J. Phys., Sect. B **25**, 1362 (1975).
- ¹¹T. Shirahata, M. Kibune, H. Yoshino, and T. Imakubo, Chem.-Eur. J. **13**, 7619 (2007).
- ¹²H. Sawa, E. Ninomiya, T. Ohama, H. Nakao, K. Ohwada, Y. Murakami, Y. Fujii, Y. Noda, M. Isobe, and Y. Ueda, J. Phys. Soc. Jpn. **71**, 385 (2002).
- ¹³K. Ohwada, Y. Fujii, Y. Katsuki, J. Muraoka, H. Nakao, Y. Murakami, H. Sawa, E. Ninomiya, M. Isobe, and Y. Ueda, Phys. Rev. Lett. **94**, 106401 (2005).
- ¹⁴H. Urayama, H. Yamochi, G. Saito, K. Nozawa, T. Sugano, M. Kinoshita, S. Sato, K. Oshima, A. Kawamoto, and J. Tanaka, Chem. Lett. **1988**, 55.
- ¹⁵A. A. Galimzyanov, A. A. Ignat'ev, N. D. Kushch, V. N. Laukhin, M. K. Makova, V. A. Merzhanov, L. P. Rozenberg, R. P. Shibaeva, and E. B. Yagubskii, Synth. Met. **33**, 81 (1989).
- ¹⁶P. Le Maguerès, L. Ouahab, N. Conan, C. J. Gómez-García, P. Dellhaès, J. Even, and M. Bertault, Solid State Commun. **97**, 27 (1996).
- ¹⁷A. Ota, L. Ouahab, S. Golhen, Y. Yoshida, M. Maesato, G. Saito, and R. Świetlik, Chem. Mater. **19**, 2455 (2007).
- ¹⁸R. Świetlik, M. Polomska, L. Ouahab, and J. Guillevic, J. Mater. Chem. **11**, 1313 (2001).
- ¹⁹T. Mori, A. Kobayashi, Y. Sasaki, H. Kobayashi, G. Saito, and H. Inokuchi, Bull. Chem. Soc. Jpn. **57**, 627 (1984). The atomic orbital parameters we used are in Ref. 20.
- ²⁰T. Mori and M. Katsuhara, J. Phys. Soc. Jpn. **71**, 826 (2002).
- ²¹G. F. Koster, Solid State Phys. **5**, 173 (1957).
- ²²K. Oshima, T. Mori, H. Inokuchi, H. Urayama, H. Yamochi, and G. Saito, Phys. Rev. B **38**, 938 (1988).
- ²³G. Burns, *Introduction to Group Theory with Applications* (Academic, New York, 1977).
- ²⁴T. Kawamoto, T. Mori, T. Yamaguchi, T. Terashima, S. Uji, T. Shirahata, M. Kibune, H. Yoshino, and T. Imakubo (unpublished).
- ²⁵J. D. Axe, A. H. Moudden, D. Hohlwein, D. E. Cox, K. M. Mohanty, A. R. Moodenbaugh, and Y. Xu, Phys. Rev. Lett. **62**, 2751 (1989).
- ²⁶K. Bechgaard, K. Carneiro, F. B. Rasmussen, M. Olsen, G. Rindolf, C. S. Jacobsen, H. J. Pedersen, and J. C. Scott, J. Am. Chem. Soc. **103**, 2440 (1981).
- ²⁷J. P. Pouget, G. Shirane, K. Bechgaard, and J. M. Fabre, Phys. Rev. B **27**, 5203 (1983).